carried out using coplanar-waveguide technology. Table 1 shows an example of a 3dB branch-line hybrid terminated by arbitrary impedances as shown in Fig. 1. As this 3dB branch-line hybrid is not terminated by 50Ω impedances, additional matching-transformer lines are indispensable for measuring. Z_{o1}, Z_{o2}, Z_{o3} and Z_{o4} in Table 1 are transformer-line characteristic impedances and their experimental data are shown in Table 1. Also, termination impedance constants (which indicate termination admittances), the experimental data of branch-line characteristic impedance, Z_1, Z_2, Z_3 and Z_4 are shown in Table 1. This 3dB branch-line hybrid terminated by arbitrary impedances was fabricated on Al_2O_3 substrate (ε_r = 10 and h = 635μm) using coplanar technology, and designed at a centre frequency of 3GHz.

A comparision between simulated and measured results for this branch-line hybrid is given in Fig. 2. For the simulation of this uniplanar 3dB branch-line hybrid, HP-EEsof series IV was used as a simulator. Fig. 2*a* shows the simulation responses with the values $|S_{21}|$ = –3.010, $|S_{31}|$ = –3.060, $|S_{11}|$ = –36.487 and $|S_{41}|$ = –33.914dB at the centre frequency of 3GHz. The experimental results of this uniplanar branch-line hybrid in the case of port 1 excitation are shown in Fig. 2*b*.

The theoretical value of the dielectric constant is 10. However, the centre frequency of the measured results is shifted to a higher frequency, as seen in Fig. 2*b*. This means that the real value of the effective dielectric constant is smaller than the theoretical value by the equation, $f_x/f_o \propto \sqrt{\varepsilon_{oe}}/\sqrt{\varepsilon_{xe}}$, where ε_{oe} and ε_{xe} are effective dielectric constants at the frequencies f_o and f_x.

Conclusions: In this letter, new design equations for a 3dB branch-line hybrid terminated by arbitrary impedances are presented. Using these design equations, a large reduction in the total size of integrated-microwave circuits can be obtained.

20 March 1998

Electronics Letters Online No: 19980816

H.-R. Ahn and I. Wolff (*Gerhard-Mercator-University Duisburg, FB9/ ATE Bismarckstrasse 81, D-47048, Duisburg, Germany*)

E-mail: wolff@ate.uni-duisburg.de

References

1 AHN, H.-R., WOLFF, I., and CHANG, I.-S.: 'Arbitrary termination impedances, arbitrary power division and small-sized ring hybrids', *IEEE Trans. Microw. Theory Tech.*, 1997, **MTT-45**, pp. 2241–2247

2 AHN, H.-R., CHANG, I.-S., and YUN, S.-W.: 'Miniaturized 3-dB ring hybrid terminated by arbitrary impedances', *IEEE Trans. Microw. Theory Tech.*, 1994, **MTT-42**, pp. 2216–2221

3 TYRREL, W.A.: 'Hybrid circuits for microwaves', *Proc. IRE*, 1947, **35**, pp. 1294–1306

4 REED, J., and WHEELER, G.J.: 'A method of analysis of symmetrical four-port networks', *IRE Trans. Microw. Theory Tech.*, 1956, **MTT-4**, pp. 346–352

5 YOUNG, L.: 'Synchronous branch guide directional couplers for low and high power applications', *IRE Trans. Microw. Theory Tech.*, 1962, **MTT-10**, pp. 459–475

6 REED, J.: 'The multiple branch waveguide coupler', *IRE Trans. Microw. Theory Tech.*, 1958, **MTT-6**, pp. 398–403

7 LEVY, R., and LIND, L.: 'Synthesis of symmetrical branch-guide directional couplers', *IEEE Trans. Microw. Theory Tech.*, 1968, **MTT-16**, pp. 80–89

8 MALHERBE, J.A.G.: 'Microwave transmission line couplers' (Artech House, Norwood, 1988), p. 22

9 HOWE, H.J.R.: 'Stripline circuit design' (Artech House, Norwood, 1974), pp. 76–84

10 BHARTIA, P., and BHAL, I.J.: 'Millimeter wave engineering and applications' (Wiley, New York, 1984), p. 355

Evaluation of spatial Green's functions for microstrips: fast Hankel transform algorithm and complex image method

Rong-Chan Hsieh and Jen-Tsai Kuo

The fast Hankel transform (FHT) algorithm and complex image method (CIM) are employed to evaluate the spatial-domain Green's function for a multilayered microstrip structure. The results are compared with those obtained by exact numerical integration. It is found that both techniques have high efficiency and the FHT has better accuracy than the CIM.

Introduction: Fast evaluation of the time-consuming Sommerfeld integral for the spatial-domain Green's function is a key issue in full-wave spatial-domain analysis of microstrip circuits. The fast Hankel transform (FHT) can greatly reduce this computational cost [1]. In the FHT [2], the Sommerfeld integral is reduced to a discrete convolution sum, in which the digital filter coefficient function has a fast decaying analytic expression. As a result, efficient and accurate calculations can always be achieved.

The complex image method (CIM) [3–5] is widely adopted for obtaining closed-form spatial Green's functions of planar structures. This method is at least two orders of magnitude more efficient than direct numerical integration [4]. However, the calculated Green's functions from the CIM have a limited region of validity and are sensitive to key parameters [4]. In [5], a two-level approach is proposed to overcome the difficulties in choosing the key parameters.

In this Letter, the FHT and the two-level approach are used to approximate the Green's function of a microstrip. The results obtained by these two methods are validated by direct integration. Emphasis is placed on numerical efficiency and accuracy.

Spatial-domain Green's function: (i) *FHT method*: For a microstrip structure, the spatial-domain Green's function is the Hankel transform of the spectral-domain counterpart:

$$G(\rho) = \frac{1}{2\pi}\int_0^\infty \tilde{G}(k_\rho) J_0(k_\rho \rho) k_\rho \, dk_\rho \qquad (1)$$

which is known as the Sommerfeld integral. It is highly oscillatory and computationally expensive. The FHT has been proven [1, 2] to be an efficient technique for evaluating $G(\rho)$ in eqn. 1. The procedure is summarised as follows. The surface wave poles (SWPs) and the LSE and LSM parallel-plate waveguide mode poles (WGPs) are extracted from $\tilde{G}(k_\rho)$ and evaluated by the residue calculus. The remaining spectral function $\tilde{G}_r(k_\rho)$ is then a smooth function. The FHT algorithm is applicable to reduce eqn. 1 with $\tilde{G}_r(k_\rho)$ to a discrete convolution form. The high efficiency and accuracy of the FHT algorithm are achieved due to the facts that (i) the digital filter coefficient function has an analytic and quickly convergent expression, and (ii) the filter length and sampling density can be optimised. Two thirds of the length of the digital filter can be further reduced if an appropriate sampling shift is introduced.

(ii) *Two-level CIM*: In the two-level CIM [5], the complex images are obtained in two successive stages. The approximation parameters in each stage are independently chosen according to the spectral-domain function behaviour. This makes the method itself numerically efficient. It is not necessary, before the two-level approximation is used, to extract the quasi-static images and SWPs from the spectral-domain function, as remarked in [5]. However, it is known that the contributions from the SWPs and WGPs may become dominant beyond a certain distance range. Therefore, when the number of dielectric layers is small, it would be better to extract these poles from the spectral-domain function, before the use of the two-level approach, for calculating $G(\rho)$ over a large distance range. The two-level approaches without and with the pole-extraction preprocess are denoted as CIM (A) and CIM (B), respectively, herein.

Comparison of FHT and CIM: Fig. 1 compares the normalised vector potential Green's functions $G_A(\rho)$ obtained by the FHT and the CIM with those obtained by exact integration of the referred results, at F = 20, 40 and 80GHz. In the FHT, 60 samples per decade of ρ/λ_0 are used and the CPU time for a Pentium-II PC to

compute each of the three curves is ~ 0.5s. In the CIM [5], the sampling ranges are $T_{01} = 400$ and $T_{02} = 5$, the numbers of complex images are $N_1 = 5$ and $N_2 = 8$, and the numbers of sampling points are $N_{s1} = 50$ and $N_{s2} = 100$. These parameters have been shown to be suitable for any Green's function without any trial step. The computation time for each curve is ~ 0.3s.

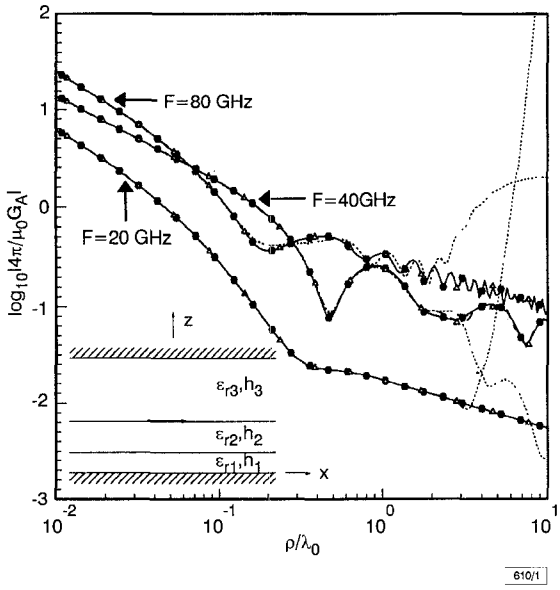

Fig. 1 *Normalised vector potential Green's function of electric dipole*

Parameters: $\varepsilon_{r1} = 10.2$, $h_1 = 0.508$mm, $\varepsilon_{r2} = 2.2$, $h_2 = 0.254$mm, $\varepsilon_{r3} = 1.0$, $h_3 = 9.238$mm
——— exact numerical integration
—·—· FHT
····· CIM (A)
—△— CIM (B)

In Fig. 1, both the FHT and the CIM (B) results show excellent agreement with the exact integrations, while the CIM (A) curves start to deviate from the referred results at $\rho/\lambda_0 = 3$, 0.4 and 0.1 for $F = 20$, 40 and 80GHz, respectively.

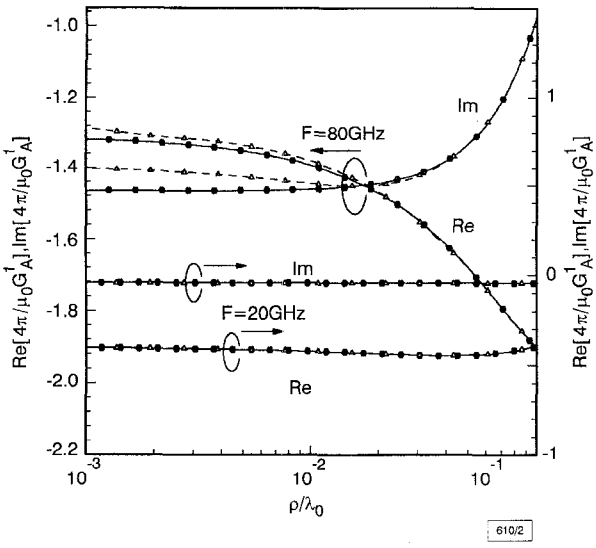

Fig. 2 *Normalised partial vector potential Green's function (G_A^1) (F = 20 and 80GHz)*

——— exact numerical integration
—·—· FHT
—△— CIM (B)

It is known that $G_A(\rho)$ is dominated by an analytic ρ^{-1} term in the near field region. Therefore, it is beneficial for circuit analysis purposes to separate it from the full Green's function $G_A(\rho)$

$$G_A(\rho) = \frac{\mu_0}{4\pi\rho} + G_A^1(\rho) \qquad (2)$$

Fig. 2 shows the normalised partial Green's function $(4\pi/\mu_0)G_A^1(\rho)$ for the region $\rho/\lambda_0 \leq 0.1$. The function value approaches a constant as ρ approaches zero. All the FHT results agree quite well with the referred results. The CIM (B) results at 20GHz are also indistinguishable from the referred results. The situation deteriorates as the frequency is increased to 80GHz. The CIM (B) results start to deviate from the referred results as $\rho/\lambda_0 \leq 0.01$ and the deviations are 2.4 and 4.3% for the real and imaginary parts, respectively, at $\rho/\lambda_0 = 0.001$. This can be improved by increasing the numbers of complex images N_1 and N_2. For example, if $N_1 = 10$ and $N_2 = 16$, the deviations will reduce to 0.4 and 1.9% for the real and imaginary parts, respectively.

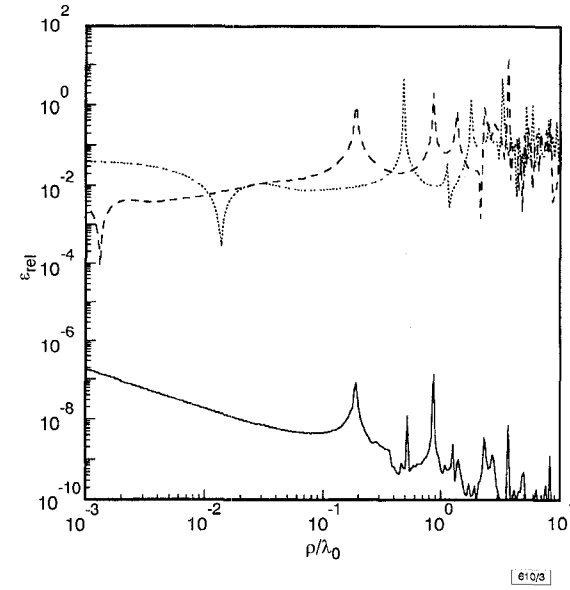

Fig. 3 *Relative error ε_{rel} of calculated FHT and CIM (B) results (F = 40GHz)*

——— $\mathrm{Re}[G_A^1]$, FHT
– – – – $\mathrm{Re}[G_A^1]$, CIM (B)
····· $\mathrm{Im}[G_A^1]$, CIM (B)

Fig. 3 compares the relative accuracy of the FHT and CIM (B) calculations with respect to the referred results at 40GHz. For the FHT calculations, only the real parts need investigating here, since the imaginary parts are completely made up from the SWPs and GWPs, which are already treated as an exact solution. As indicated, the maximum ε_{rel} for the FHT data is $< 10^{-6}$, while the minimum ε_{rel} for the CIM (B) results is 10^{-4}.

Conclusion: Both the fast Hankel transform (FHT) and complex image method (CIM) are efficient in evaluating the spatial-domain Green's function for microstrip structures. For the particular case study shown, for $10^{-3} \leq \rho/\lambda_0 \leq 10$, the accuracy of the FHT is better than that of the CIM.

25 March 1998
Electronics Letters Online No: 19980787

Rong-Chan Hsieh and Jen-Tsai Kuo (*Department of Communication Engineering, National Chiao Tung University, 1001 Tahsueh Road, Hsinchu, 300 Taiwan, Republic of China*)

E-mail: jtkuo@cmhp22.cm.nctu.edu.tw

References

1 HSIEH, R.C., and KUO, J.T.: 'Fast full-wave characterization of arbitrary planar microstrip geometries'. Asia Pacfic Microwave Conference, December 1997, Hong Kong, pp. 685–688
2 CHRISTENSEN, N.B.: 'Optimized fast Hankel transform filters', *Geophys. Prospect.*, 1990, **38**, pp. 545–568
3 CHOW, Y.L., YANG, J.J., FANG, D.H., and HOWARD, G.E.: 'A closed-form spatial Green's function for the thick microstrip substrate', *IEEE Trans. Microw. Theory Tech.*, 1991, **MTT-39**, pp. 588–592
4 WEBB, D.B., and MITTRA, R.: 'Practical implementation of the complex image method for the solution of nonplanar multilayered media problems'. Proc. IEEE-APS Int. Symp., July 1996, Baltimore, Maryland, pp. 420–423
5 AKSUN, M.I.: 'A robust approach for the derivation of closed-form Green's functions', *IEEE Trans. Microw. Theory Tech.*, 1996, **MTT-44**, pp. 651–658